

Published in final edited form as:

Chem Sci. 2011 February 1; 2011(2): 273–278. doi:10.1039/C0SC00297F.

## Borrelidin modulates the alternative splicing of VEGF in favour of anti-angiogenic isoforms

Jeanette Woolard<sup>b</sup>, William Vousden<sup>a</sup>, Steven J. Moss<sup>a</sup>, Arjun Krishnakumar<sup>b</sup>, Melissa VR Gammons<sup>b</sup>, David G Nowak<sup>b</sup>, Neil Dixon<sup>d</sup>, Jason Micklefield<sup>d</sup>, Astrid Spannhoff<sup>e</sup>, Mark T. Bedford<sup>e</sup>, Matthew A. Gregory<sup>a</sup>, Christine J. Martin<sup>a</sup>, Peter F. Leadlay<sup>c</sup>, Ming Q. Zhang<sup>a</sup>, Steven J. Harper<sup>b</sup>, David O. Bates<sup>b</sup>, and Barrie Wilkinson<sup>a</sup>

<sup>a</sup>Biotica, Chesterford Research Park, Cambridge, CB10 1XL, UK. Fax: +44 (0)1799 532921; Tel: +44 (0)1799 532925; barrie.wilkinson@biotica.com

<sup>b</sup>Microvascular Research Laboratories, Bristol Heart Institute, Department of Physiology and Pharmacology, School of Veterinary Sciences, University of Bristol, Southwell Street Bristol, BS2 8EJ, UK. Fax: +44 (0)117 9288151; Tel: +44 (0)117 9289818; dave.bates@bristol.ac.uk

<sup>c</sup>Department of Biochemistry, 80 Tennis Court Road, University of Cambridge, Cambridge CB2 1GA, UK

<sup>d</sup>School of Chemistry and Manchester Interdisciplinary Biocentre, University of Manchester, 131 Princess Street, Manchester, M1 7DN, UK

<sup>e</sup>The University of Texas M.D. Anderson Cancer Center, Science Park-Research Division, Smithville, Texas 78957, USA

### Abstract

The polyketide natural product borrelidin **1** is a potent inhibitor of angiogenesis and spontaneous metastasis. Affinity biopanning of a phage display library of colon tumor cell cDNAs identified the tandem WW domains of spliceosome-associated protein formin binding protein 21 (FBP21) as a novel molecular target of borrelidin, suggesting that borrelidin may act as a modulator of alternative splicing. In support of this idea, **1**, and its more selective analog **2**, bound to purified recombinant WW domains of FBP21. They also altered the ratio of vascular endothelial growth factor (VEGF) isoforms in retinal pigmented endothelial (RPE) cells in favour of anti-angiogenic isoforms. Transfection of RPE cells with FBP21 altered the ratio in favour of pro-angiogenic VEGF isoforms, an effect inhibited by **2**. These data implicate FBP21 in the regulation of alternative splicing and suggest the potential of borrelidin analogs as tools to deconvolute key steps of spliceosome function.

### Introduction

We previously reported the mutasynthesis<sup>1</sup> of new analogs of the anti-bacterial<sup>2</sup> and anti-angiogenic<sup>3,4</sup> polyketide borrelidin **1** using genetically engineered strains of the producing organism *Streptomyces parvulus* Tü4055. Of particular note was BC194 **2** which exhibits markedly reduced cytotoxic effects and a significantly enhanced ability (pM rather than nM)

© The Royal Society of Chemistry [year]

Correspondence to: David O. Bates; Barrie Wilkinson.

†Electronic Supplementary Information (ESI) available: General chemical methods; natural products & synthetic chemistry; isothermal titration calorimetry data; *in vitro* HUVEC anti-angiogenesis assays; correction of the FBP21 cDNA expression vector. See DOI: 10.1039/b000000x/

to inhibit *in vitro* models of angiogenesis.<sup>6</sup> **2** differs from **1** only in the cyclopentanecarboxylic acid moiety which is truncated to a cyclobutanecarboxylic acid. Modulation of the *in vitro* toxicity to angiogenesis inhibition profile of **1** was also reported for analogs where the carboxylic acid moiety was modified synthetically.<sup>7</sup> Taken together these data suggest that modifications in this region confer selectivity. **1** exhibits additional biological activities of interest including potent inhibition of spontaneous metastasis *in vivo*,<sup>4</sup> and of cell migration *in vitro*.<sup>8</sup>

The antibacterial action of **1** is exerted uniquely through inhibition of threonyl-tRNA synthetase<sup>9</sup> (ThrRS) but several poorly-understood mechanisms appear to be involved in its anti-angiogenic activity.<sup>3,5,10</sup> It is probable that **1** inhibits mammalian ThrRS<sup>11</sup> but this has not been verified at the biochemical level. In this article we report our efforts to identify the putative molecular target of **1** responsible for its potent anti-angiogenic activity and subsequent biological evaluation.

## Results and Discussion

To help clarify the molecular target(s) responsible for its anti-angiogenic activity we coupled **1** and its biosynthetically-engineered<sup>1</sup> analog **3**, which is inactive in *in vitro* assays of angiogenesis<sup>5</sup> and cell proliferation<sup>1,5</sup> inhibition, to biotin in order to enable immobilization on streptavidin coated surfaces. This was achieved by activation of the carboxylic acid as a mixed-anhydride (treatment with isobutylchloroformate and dimethylaminopyridine), followed by reaction with biotinamidohexanoic acid hydrazide to yield **4** (from **1**) and **5** (from **3**) (see Fig. 1 and ESI). The use of **3** provides a negative control against which to compare **1**. As modification of the carboxylic acid moiety enhances selectivity *in vitro*, we anticipated an enrichment for angiogenesis inhibition related targets using affinity methods of selection.

The resulting probes were used as bait for the biopanning of a T7Select cDNA phage display library derived from a human colon cancer cell line (Novagen) expressed in *Escherichia coli* BLT5403. This method has been used successfully with other natural products<sup>11,12</sup>. After four rounds of biopanning with **4**, the amplified lysate was split and two fifth round biopanning experiments were performed in parallel, one using SDS elution (as used for rounds 1-4) and the other using elution by *E. coli* cells which has been suggested to increase the likelihood of identifying weak target:ligand binding interactions.<sup>12</sup> This procedure resulted in the progressive enrichment of two phage products of approximately 450 and 600 basepairs as shown by PCR amplification of the complete phage pool eluted after each round of biopanning (Fig. 2a). For each fifth round elution experiment DNA from 12 individual phage plaques was amplified using PCR (Fig. 2b), sequenced and compared with published databases to identify the displayed protein fragments. Two out of the SDS-eluted phage contained a cDNA insert encoding a sequence encoding 99 amino acids in frame with the phage coat protein, of which a region of 83 residues was identical with human formin binding protein 21 (FBP21) (Fig. 2c). Strikingly, this protein fragment corresponds exactly to the tandem WW domains of FBP21, a structural motif likely to mediate specific protein-protein interactions.<sup>13</sup> Of the remaining 10 SDS-eluted phage, none found a significant match in sequence databases. Most displayed 20 amino acids or less, and were disregarded as background binders, while the others were eliminated as they contained open reading frames reversed with respect to the direction of expression, or predicted a protein not in-frame with the phage coat protein. Of the *E. coli*-eluted phage, 10 contained the same FBP21 insert (see Fig. 2b). The remaining clones contained a cDNA insert of less than 150 bp in length that generated no BLAST hits. As a control, identical experiments were performed using **5** as bait. This gave a very different amplification pattern, and none of the

phage contained FBP21 encoding inserts. When repeated, all experiments gave essentially the same results.

FBP21 is a known splicing factor.<sup>13</sup> The WW domains of FBP21 are similar to those of yeast splicing factor PRP40, and FBP21 is present in highly purified spliceosomal complex A. It co-localizes with splicing factors in nuclear speckles, and interacts directly with U1 snRNP protein U1C, the core snRNP splicing factors SmB and SmB', and the branch point binding-protein SF1/mBBP, strongly suggesting that FBP21 plays a role in the cross-intron bridging of U1 and U2 snRNPs in the mammalian A complex. Recent studies have shown that FBP21 also interacts with SIPP1 (splicing factor that interacts with PQBP1 and PP1) *in vitro* and *in vivo*, and targeted mutagenesis has confirmed that these interactions are mediated by the tandem WW domains.<sup>14</sup> Formin binding proteins (FBPs) and other WW domain-encoding proteins are increasingly viewed as scaffolding proteins which provide a platform for the exchange of spliceosome-associated splicing factors and other proteins.<sup>15,16</sup> For example, the WW domain-containing proteins CA150 and FBP11 are known to associate with U2 snRNP, splicing factors SF1, U2AF and components of the SF3 complex,<sup>15</sup> indicating that WW domain-associating factors bind to the 3' part of an intron during spliceosome assembly. It was additionally shown that such effects can modulate alternative exon selection by facilitating particular 3' splice site recognition, an effect apparently specific to selection of the 3' site. Identification of the WW domains of FBP21 as a potential molecular target of **1** raised the exciting possibility that inhibition of pre-mRNA splicing, and/or the modulation of alternative splicing, might account for at least part of the anti-angiogenic effect of this compound. Natural products have repeatedly shown their value as selective inhibitors/modulators/identifiers of cellular processes,<sup>17</sup> and several natural products of polyketide origin have recently been reported as inhibitors of the spliceosome.<sup>18</sup>

To measure directly the binding of **1** and **2**, a fragment of FBP21 (amino acids 129-197 of NP\_061235.2) housing the tandem WW domains was expressed and purified as a GST fusion protein as described previously.<sup>19</sup> This fragment has been shown competent in binding various splicing factors, and utilized in a range of assays.<sup>13</sup> The affinity of **1** and **2** was measured using isothermal titration calorimetry (ITC). Binding of both compounds was associated with only a small change in enthalpy, and was driven by favourable entropic effects (see ESI). This entropic binding is consistent with a hydrophobic binding interaction at the ligand-protein interface, whereby the binding is presumably driven by desolvation of **1** and **2**. Because the enthalpy changes associated with these interactions were small, optimal signal to noise ratios were obtained for experiments conducted at 15°C. **1** and **2** gave dissociation constants ( $K_d$ ) under these conditions of  $11.8 \pm 2.7 \mu\text{M}$  and  $9.7 \pm 3.1 \mu\text{M}$  respectively. The affinity of the control peptide SMB<sup>20</sup> was  $16.4 \pm 1.9 \mu\text{M}$  under these conditions, and in contrast is entirely driven by enthalpy.

To explore the effect of **1** and analogs on alternative pre-mRNA splicing we focused on VEGF, a key regulator of physiological and pathological angiogenesis, which is organized as eight exons and exists in multiple isoforms generated by alternative pre-mRNA splicing.<sup>21</sup> A C-terminal splicing event in the VEGF mRNA results in production of two families of VEGF isoforms, termed VEGF<sub>xxx</sub> and VEGF<sub>xxx</sub>b which are formed by use of alternative 3' acceptor splice sites in exon 8, 66-bp apart. In both families of isoforms, alternative splicing results in proteins with identical numbers of amino acid residues but the mRNAs differ in an 18 base open reading frame encoding for either the pro-angiogenic (exon 8a) Cys-Asp-Lys-Pro-Arg-Arg or the anti-angiogenic (exon 8b) Ser-Leu-Thr-Arg-Lys-Asp at the C-terminus.<sup>22,23</sup> In contrast to the VEGF<sub>xxx</sub> family, which is potently pro-angiogenic, the VEGF<sub>xxx</sub>b family of proteins has anti-angiogenic activity and inhibits VEGF-mediated activation of VEGFR2 and tumour growth *in vivo*.<sup>23,24</sup> VEGF<sub>xxx</sub>b isoforms are expressed in most tissues and by many cell types including retinal cells and can

be differentially regulated in angiogenic conditions such as diabetic retinopathy<sup>25</sup> and cancer.<sup>26</sup> Thus, the expression ratio of these isoforms correlates strongly with the angiogenic status of cell types and is differentially regulated by splicing and growth factors.<sup>27</sup>

The effect of **1-3** on VEGF alternative splicing was examined in primary retinal pigmented endothelial (RPE) cells which express both VEGF<sub>xxx</sub> and VEGF<sub>xxx</sub>b isoforms (where xxx is used to denote the number of amino acids in the resulting protein, e.g. VEGF<sub>165</sub>, VEGF<sub>121</sub>b, or VEGF<sub>165</sub>b).<sup>27</sup> RPE cells were treated with compounds and the culture medium analyzed after 72 h using an ELISA method as described previously.<sup>27</sup> At concentrations of 0.5 and 5  $\mu$ M **1** and **2** significantly decreased the expression of VEGF<sub>xxx</sub> isoforms whilst increasing the expression of VEGF<sub>xxx</sub>b isoforms (Fig. 3ab). The VEGF<sub>xxx</sub>b isoform predominantly expressed was VEGF<sub>165</sub>b although VEGF<sub>121</sub>b was also seen at a lower level. The inactive compound **3** had no effect, even at 5  $\mu$ M. Upon treatment with increasing concentrations of **2** RPE cells showed a concentration-dependent decrease in expression of VEGF<sub>xxx</sub> (calculated from the difference between total VEGF and VEGF<sub>xxx</sub>b) and a concomitant increase in VEGF<sub>xxx</sub>b (Fig. 3c) (**2** was used in preference to **1** here and in further studies described due to its lower toxicity to RPE cells). VEGF<sub>165</sub>b competitively antagonises VEGF<sub>165</sub>-mediated endothelial proliferation, migration and angiogenesis at or above a 1:1 molar ratio.<sup>28</sup> A value >1 represents a pro-angiogenic cellular environment, whilst a value <1 represents an anti-angiogenic environment. A VEGF<sub>165</sub>:VEGF<sub>165</sub>b molar ratio of 5 should be sufficient to support angiogenesis, and a value of 0.2 sufficient to block angiogenesis completely.<sup>23</sup> As shown in Figure 3c treatment with **2** at 0.5  $\mu$ M shifted this ratio to a clearly anti-angiogenic value (<1). It is noteworthy that the amide analog **6** proved to be as effective as **1** and **2** in stimulating VEGF<sub>xxx</sub>b protein expression, confirming that modification of the carboxylic acid group, as in the biotinylated probes **4** and **5**, does not compromise the activity of the compound in modulating splicing.

Treatment of RPE cells with insulin-like growth factor-1 (IGF-1) (1  $\mu$ M) upregulates VEGF<sub>165</sub>, by inducing proximal splice site selection.<sup>27</sup> When **2** was co-administered at several concentrations with IGF-1 it completely abolished this effect upon VEGF<sub>165</sub> protein expression (Fig. 3d), showing that proximal splice site selection in the VEGF gene induced by IGF-1 was being inhibited. The lack of upregulation of any VEGF isoform by IGF-1 in the presence of **2** indicates that IGF was prevented from stimulating selection of the proximal splice site. To further probe the interaction between **2** and FBP21, we transfected RPE cells with the FBP21 cDNA expression plasmid pWV327, a pCMV6 based vector for expression of full-length FBP21 (see ESI). RPE cells transfected with pWV327 produced significantly less 85 VEGF<sub>165</sub>b (0.36 $\pm$ 0.03 pg/ $\mu$ g protein) than cells transfected with the control vector (0.49 $\pm$ 0.03 pg/ $\mu$ g protein,  $p$ <0.05; Fig. 4a). The upregulation of VEGF<sub>165</sub>b by **2** seen in control cells (2.9 $\pm$ 0.78 fold) was reduced by transfection with FBP21 (1.8 $\pm$ 0.15 fold,  $p$ =0.05), indicating that the response to **2** is likely to be FBP21-dependent (Fig. 4b). An FBP21-dependent response to **2** is consistent with the concept that it acts through direct binding to FBP21, although a more indirect effect cannot be completely excluded.

## Conclusions

The modulation of VEGF alternative splicing in RPE cells by **2** was both reproducible, statistically significant, and dose dependent. Moreover, analog **3**, which is neither cytotoxic nor an inhibitor of angiogenesis *in vitro*, was not active in this assay. It is important to note, however, that the ability of **1** and **2** to modulate VEGF splicing requires  $\mu$ M concentrations which are significantly higher than those required for anti-angiogenic activity measured previously by monitoring capillary and tubule formation *in vitro* (nM for **1** and pM for **2**).<sup>3,5</sup> It has been proposed that **1** operates through (at least) two distinct pathways to exert its anti-angiogenic activity, one of which appears dependent upon its known ability to inhibit, or

bind to, ThrRS.<sup>9</sup> We now propose that another pathway may be through spliceosome inhibition and/or modulation.

In the course of our studies we identified the splicing factor FBP21 as a potential molecular target of **1** through the use of affinity biopanning experiments, and confirmed that **1** and **2** bind to its tandem WW-domains at concentrations required for modulation of VEGF alternative splicing in RPE cells. It was additionally shown that expression of FBP21 in RPE cells was capable of modulating terminal exon alternative splicing, significantly lowering the levels of VEGF<sub>165b</sub>, while the upregulation of VEGF<sub>165b</sub> induced by treating RPE cells with **2** was abrogated by the expression of FBP21. Additionally, **2** potently inhibited the ability of IGF-1 to upregulate VEGF<sub>165</sub> expression through induction of proximal splice site selection.

While still preliminary, these data are consistent with a model in which FBP21 is a splicing factor, one function of which is the selection of specific terminal (exon-8) splice sites during VEGF alternative splicing, and that **1** and **2** can modulate this process through interaction with FBP21. The regulation of VEGF splicing is not well understood. Currently the only splicing factors to be implicated in terminal exon splicing of VEGF are SRp55, (which promotes distal splicing), ASF/SF2 and SRp40 (which promote proximal splicing).<sup>27</sup> Further work will be required to confirm the role of the **1**-FBP21 interaction both for VEGF and more generally at influencing the outcome of alternative splicing. It is an attractive hypothesis that concerted regulation of the switch to a pro-angiogenic state might involve alteration in splicing patterns of multiple target proteins. Great strides have been made recently in reconstituting spliceosomal activities *in vitro*,<sup>29,30</sup> and use of such *in vitro* assays should in future allow a precise evaluation of the molecular mechanisms involved in **1** action. Conversely, the use of **1** derived compounds offers the perspective of deconvoluting individual steps in the action of the spliceosome.<sup>29</sup>

The findings reported here demonstrate once again the tremendous value of natural products both as chemical tools for uncovering new and rich biology, and as lead compounds for the development of potential therapeutic agents.<sup>17</sup> Indeed, we suggest that interfering with interactions between FBP21 and its normal binding partners represents a novel pharmacological target. It may be possible in the future to obtain **1**-based compounds that are selective for one target over the other, e.g. FBP21 over ThrRS. We believe that detailed evaluation of **2** and other analogs is warranted as a source of potential therapeutic intervention for vascular diseases.

## Experimental procedures

### General chemical methods, natural products chemistry & chemical synthesis

These are detailed in the Electronic Supplementary Information (ESI).

### *In vitro* HUVEC anti-angiogenesis assays

Angiogenesis assays with **3** were carried out at the angiogenesis resource center of the NCI and details of the assay protocols and results are given in the ESI.

### Isothermal titration calorimetry

Purified GST-FBP fusion protein<sup>19,20</sup> was exhaustively dialysed overnight at 4°C against 100 mM phosphate saline buffer (pH 7.2 NaCl 140 mM KCl 2.7 mM). Stock solutions of SMB, **1** and **2**, were lyophilised/evaporated and re-dissolved in the exact same dialysis buffer. Samples were degassed and ITC performed at 15°C using a VP-ITC microcalorimeter (Microcal, Inc). SMB, **1** and **2** were titrated into the sample cell containing



GST-FBP in 20 injections of 15  $\mu\text{L}$  with reference power of  $2 \text{ kcal s}^{-1}$ . Data analysis was performed using Origin 5.0 (Origin Laboratories) by the single-site binding model. The fitted data allows  $K_d$  and  $\Delta H$  to be determined directly, which, using the relationship  $\Delta G = -RT \ln K_a = \Delta H - T \Delta S$ , allows the entropy change ( $T\Delta S$ ) and the free energy of binding ( $\Delta G$ ) to be calculated. The data obtained are presented in the ESI.

### Biopanning of cDNA phage display library

Streptavidin wells were incubated with  $1 \mu\text{M}$  of probe at  $4 \text{ }^\circ\text{C}$  overnight to prepare the wells for biopanning. After incubation, unbound biotinylated probe was removed from the well by washing with phosphate buffered saline (PBS). Wells were then blocked with blocking solution (3% skimmed milk in PBS) for at least one hour at room temperature. Blocked wells were then briefly washed with PBS and were ready for biopanning use. The Novagen T7 colon cancer cell line cDNA phage library was amplified using standard techniques (see Novagen T7Select™ manual provided with Novagen phage library) and stored either in  $0.5 \text{ M NaCl}$  at  $4 \text{ }^\circ\text{C}$  (for short term storage) or in 8% glycerol at  $-80 \text{ }^\circ\text{C}$  (for long term storage).

Amplified phage libraries were titered using standard techniques and were found to contain an average of  $5 \times 10^{10}$  plaque forming units per mL ( $\text{pfu mL}^{-1}$ ). In the first round of biopanning, amplified phage library ( $0.15 \text{ mL}$ ) was added to an empty streptavidin coated well and incubated at room temperature for at least 1 h. This step was included to deselect any phage displaying streptavidin binding proteins. After incubation, the phage were removed from the well and mixed with 4x blocking solution (12% skimmed milk in PBS) ( $50 \mu\text{L}$ ) and incubated at room temperature for at least 1 h.

Blocked phage library ( $125 \mu\text{L}$ ) was added to each pre-prepared biotinylated well and incubated at room temperature for at least 1 h. The supplied library contains an estimated  $1.7 \times 10^7$  distinct primary recombinant phage clones so  $>200$  copies of each clone were added to the well. After incubation unbound phage were removed from the well with wash solution. The wash solution was varied depending on the round of biopanning. For the first round of biopanning PBS1 was used. For subsequent rounds the stringency of the wash was increased by using sequentially PBS2, PBS3 and PBS4: PBS1 (round 1), 150 mM NaCl, 0.1% Tween20 in PBS; PBS2 (round 2), 170 mM NaCl, 0.3% Tween20 in PBS; PBS3 (round 3), 200 mM NaCl, 0.5% Tween20 in PBS; PBS4 (round 4), 250 mM NaCl, 0.7% Tween20 in PBS. During the first biopanning round, ten washes were performed with PBS1 followed by five washes with PBS to remove all traces of Tween20 and NaCl from the well. Similarly for subsequent rounds ten washes were performed with the appropriate wash solution followed by 5 washes with PBS. After rounds 1-4 the wells were eluted with SDS elution solution: 1% SDS in PBS ( $100 \mu\text{L}$ ) was added to the well and incubated at room temperature for at least 1 h. The eluent was then removed from the well and pipetted into *E. coli* BLT5403 grown in 2xTY media to an  $\text{OD} = 0.4$  ( $50 \text{ mL}$  in a  $250 \text{ mL}$  conical flask). The flask was incubated at  $37 \text{ }^\circ\text{C}$  with shaking at  $250 \text{ rpm}$  for approximately 4 h or until complete lysis had occurred. The lysate was transferred to a  $50 \text{ mL}$  falcon tube, solid NaCl was added to a final concentration of  $0.5 \text{ M}$ , and the lysate was centrifuged at  $4000 \text{ rpm}$  for 10 min. The supernatant was transferred to a new  $50 \text{ mL}$  tube and was stored at  $4 \text{ }^\circ\text{C}$  or used in a subsequent round of biopanning.

Two different elution techniques were employed to remove bound phage from the wells in round 5. (a) SDS elution: SDS elution solution (1% SDS in PBS) ( $100 \mu\text{L}$ ) was added to the well and incubated at room temperature for at least 1 h; or (b) *E. coli* elution:<sup>12</sup> *E. coli* elution solution (the host *E. coli* strain (BLT5403) grown to  $\text{OD} = 0.4$ ) ( $100 \mu\text{L}$ ) was added to the well and incubated at room temperature for at least 1 h. In each case the eluant was treated as described above.

Lysates from the separate round 5 panning experiments were serially diluted, mixed with *E. coli* culture (BLT5403 grown overnight at 37 °C) (250 µL), mixed with melted top agarose (3 mL, pre-equilibrated to 45 °C) and poured onto a pre-warmed plate of 2TY agar. Plates were incubated at 37 °C for 2-4 h until a bacterial lawn containing phage plaques was seen. Twelve individual phage plaques from each round 5 experiment were cut from the plates and placed into tubes containing PBS (200 µL). Tubes were vortexed briefly to liberate the phage from the agar plug. Each phage plaque suspension (1 µL) was then used as the template in a PCR reaction using T7SelectUP: 5'-GGAGCTGTCGTATTCCAGTC and T7SelectDOWN: 5-AACCCCTCAAGACCCGTTTA primers, Taq DNA polymerase and the following PCR program: 1 cycle: 80 °C for 10 min; 30-35 cycles: 94 °C for 1 min, 55 °C for 1 min, 72 °C for 2 min. The resulting PCR products were cleaned and sequenced with T7SelectUP and T7SelectDOWN oligos and the resultant data were submitted for nucleotide BLASTN searches on the NCBI website. Predicted displayed amino acid sequences were submitted to BLASTP.

### Retinal pigmented endothelial cell culture

Human retinal pigmented epithelial (RPE) cells (obtained from ATCC, Teddington, UK), are well-characterised and constitutively express both VEGF<sub>165</sub> and VEGF<sub>165b</sub>.<sup>25</sup> Cells were routinely subcultured in DMEM:F12 (1:1) media supplemented with 10% foetal bovine serum (FBS) and trypsinised with a trypsin/EDTA solution (Sigma) between passages 20-30. Once a confluency of 70-80% was achieved, RPE cells were plated in 6 well plates. To determine the effects of borrelidin or its analogs, cells were cultured in fresh medium in the absence of FBS for 24 h prior to stimulation. Both borrelidin and analogs were prepared in 2 mL of serum-free medium, at the concentrations indicated in the text. Cell number was assessed following stimulation. No changes in cell morphology were apparent upon visualisation of the cells following stimulation with borrelidin or its analogues. Following treatment with borrelidins, conditioned media was collected and stored at -20 °C until analysis by ELISA or Western Blotting. Subsequently, cells were washed with ice-cold 1XPBS and lysed in 50 µL RIPA buffer containing a protease inhibitor cocktail (Sigma, UK).

### Conditioned media and cell lysate VEGF measurements

Total pan VEGF concentrations of neat RPE conditioned medium and cell lysates were measured according to the manufacturer's instructions using a standard DuoSet VEGF ELISA (R&D Systems Cat No.DY293BE). VEGF<sub>xxx</sub>b was determined with a similar sandwich ELISA (R&D Systems Cat. No. MAB3045). For the VEGF<sub>xxx</sub>b ELISA, the capture antibody was a monoclonal biotinylated mouse anti-human antibody raised against the terminal nine amino acids of VEGF<sub>165b</sub> (R&D Systems); a standard curve for this assay was built with recombinant human VEGF<sub>165b</sub> (R&D Systems). This antibody has been characterised previously<sup>23,25</sup> and specifically detects the VEGF<sub>xxx</sub>b family of isoforms but not the conventional VEGF<sub>xxx</sub> isoforms.

### Western blotting

Cell lysate samples were quantified using the Bradford Assay for protein quantification (Biorad, UK). Samples were dissolved in loading buffer containing Tris 1M (pH 6.8), 10% SDS, 30% Glycerol, 10% Bromophenol Blue and 5% β-mercaptoethanol, and boiled for 5 min. 30 µg protein per lane were separated by SDS/PAGE (12%) and transferred to a 0.2 µm Polyvinylidene Fluoride (PVDF) membrane. Subsequently, membranes were blocked for 60 min with 5% skimmed milk / 1XPBS - 0.05% Tween, and probed overnight at room temperature with antibodies against VEGF<sub>xxx</sub>b (in house clone 56/1; 1:250) and β-tubulin (Sigma; 1:2000) in a solution containing 2.5% skimmed milk / 1xPBS - 0.05% Tween. Membranes were washed in 0.05% 1xPBS - 0.05% Tween and then incubated with a

secondary HRP-conjugated antibody (Pierce). Immunoreactive bands were visualised using ECL reagent (Pierce) and subsequently quantified using ImageJ analysis; the resulting densities were normalized to those of  $\beta$ -tubulin (n=3).

### IGF-1 treatment experiments

RPE cells were split to six-well plates ( $1 \times 10^5$  cells per well) and grown until 95% confluent cells. Twenty-four hours before treatment cultured medium was replaced with serum free RPMI-1654 medium (Sigma) containing 1% ITS (Sigma) and 0.5% PSS (Sigma). Subsequently, the medium was replaced with fresh serum free RPMI-1610 medium (Sigma) containing 1% ITS (Sigma), 0.5% PSS (Sigma) and increasing concentrations of IGF-1 (Sigma). The conditioned media were collected 24 h or 48 h after stimulation.

### RPE transfection with FBP21 and analysis

RPE cells were grown in six-well plates, each seeded with  $3 \times 10^5$  cells and subsequently transfected with 1  $\mu$ g of pWV327 or control (empty) vector using Lipofectamine (Invitrogen). Following incubation at 37 °C for 48 h, and treatment with IGF-1 as above where stated, conditioned medium was collected and cells were lysed in buffer containing: 20 mM Tris, pH7.4, 1.5% w/v Triton X-100, 150 mM NaCl, 10% w/v glycerol and protease inhibitors cocktail (Sigma). VEGF isoforms were measured in cell lysate using ELISA. Correction of the FBP21 cDNA clone is described in the ESI.

### Supplementary Material

Refer to Web version on PubMed Central for supplementary material.

### Acknowledgments

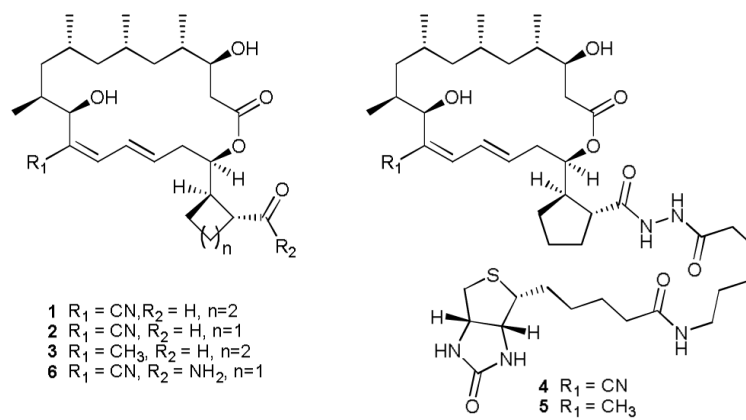
JW is funded by the Wellcome Trust (079663/Z/06/Z) and DOB by the British Heart Foundation (BS/06/005). This work was funded in part by a grant from the Richard Bright VEGF Research Trust. Mark Bedford is supported by a Welch Foundation Grant (G-1495) and a NIDA grant (DA025800). Astrid Spannhoff is supported by The German Research Foundation (SP1262/1-1).

### Notes and references

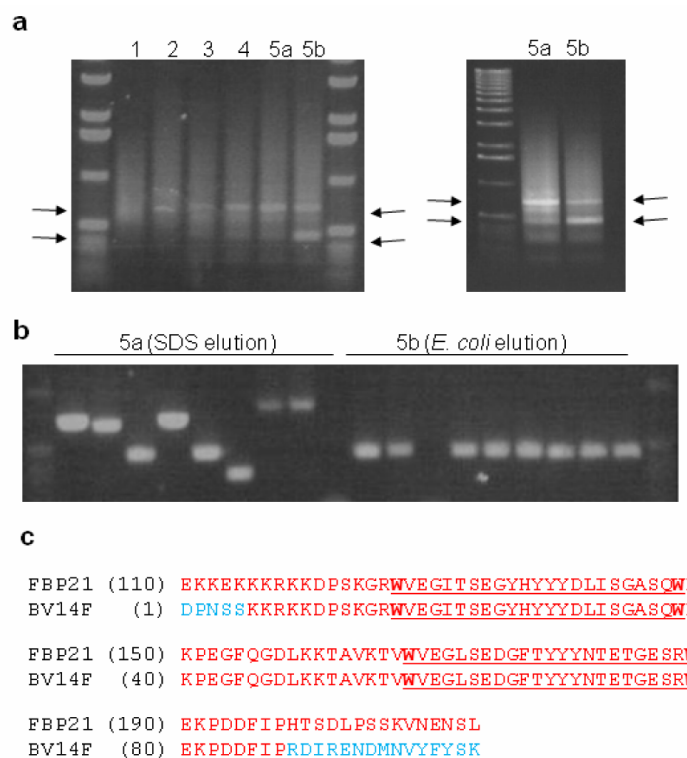
1. Moss SJ, Carletti I, Olano C, Sheridan RM, Ward M, Math V, Nur-e-Alam M, Braña AF, Zhang M-Q, Leadlay PF, Méndez C, Salas JA, Wilkinson B. *Chem. Commun.* 2006;2341–2343.
2. Buck M, Farr AC, Schnitzer RJ. *Trans. New York Acad. Sci.* 1949; 11:207–210. [PubMed: 18150150]
3. Wakabayashi T, Kagayama R, Naruse N, Tsukahara N, Funahashi Y, Kitoh K, Watanabe Y. *J. Antibiot.* 1997; 50:671–676. [PubMed: 9315080]
4. Funahashi Y, Wakabayashi T, Semba T, Sonoda J, Kitoh K, Yoshimatsu K. *Oncol. Res.* 1999; 11:319–329. [PubMed: 10757446]
5. Wilkinson B, Gregory MA, Moss SJ, Carletti I, Sheridan RM, Kaja A, Ward M, Olano C, Méndez C, Salas JA, Leadlay PF, VanGinkel R, Zhang M-Q. *Bioorg. Med. Chem. Lett.* 2006; 16:5814–5817. also see ESI. [PubMed: 16962775]
6. *PCT.*, WO 01/09112. 2001.
7. Harisi R, Kenessey I, Olah JN, Timar F, Babo I, Pogany G, Paku S, Jeney A. *Anticancer Res.* 2009; 29:2981–2985. [PubMed: 19661304]
8. Ruan B, Bovee ML, Sacher M, Stathopoulos C, Poralla K, Francklyn CS, Söll D. *J. Biol. Chem.* 2005; 280:571–577. [PubMed: 15507440]
9. Kawamura T, Liu D, Towle MJ, Kageyama R, Tsukahara N, Wakabayashi T, Littlefield BA. *J. Antibiot.* 2003; 56:709–715. [PubMed: 14563161]
10. Gerken SC, Arfin SM. *J. Biol. Chem.* 1984; 259:9202–9206. [PubMed: 6746646]



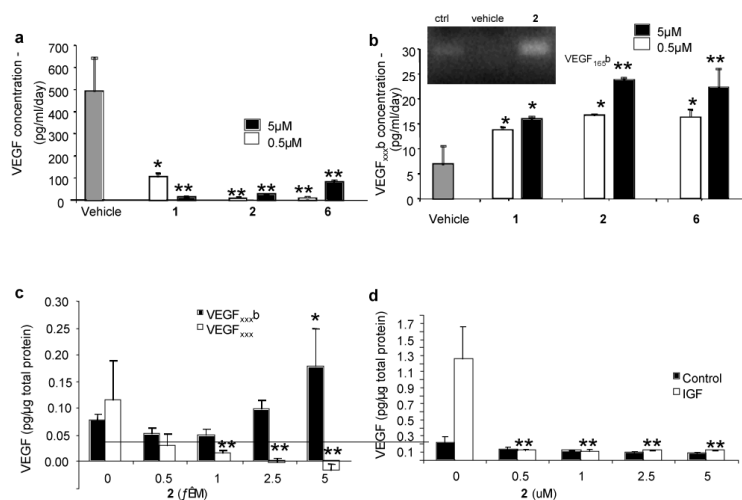
11. Kim H, Deng L, Xiong X, Hunter WD, Long MC, Pirrung MC. *J. Med. Chem.* 2007; 50:3423–3426. [PubMed: 17595071] Jin Y, Yu J, Yu Y–G. *Chem. Biol.* 2002; 9:157–162. [PubMed: 11880030]
12. McKenzie KM, Videlock EJ, Splittgerber U, Austin DJ. *Angew. Chem. Intl. Ed. Engl.* 2004; 116:4144–4147.
13. Bedford MT, Reed R, Leder P. *Proc. Natl. Acad. Sci. USA.* 1998; 95:10602–10607. [PubMed: 9724750]
14. Huang X, Beullens M, Zhang J, Zhou Y, Nicolaescu E, Lesage B, Hu Q, Wu J, Bollen M, Shi Y. *J. Biol. Chem.* 2009; 284:25375–25387. [PubMed: 19592703]
15. Lin K–T, Lu R–M, Tarn W–Y. *Mol. Cell Biol.* 2004; 24:9176–9185. [PubMed: 15456888]
16. Ingham RJ, Colwill K, Howard C, Dettwiler S, Lim CSM, Yu J, Hersi K, Raaijmakers J, Gish G, Mbamalu G, Taylor L, Yeung B, Vassilovski G, Amin M, Chen F, Matskova L, Winberg G, Ernberg I, Linding R, O'Donnell P, Starostine A, Keller W, Metalnikov P, Stark C, Pawson T. *Mol. Cell Biol.* 2005; 25:7092–7106. [PubMed: 16055720]
17. Dixon N, Wong LS, Geerlings TH, Micklefield J. *Nat. Prod. Rep.* 2007; 24:1288–1310. [PubMed: 18033580]
18. Kotake Y, Sagane K, Owa T, Minori-Kiyosue Y, Shimizu H, Uesugi M, Ishihama Y, Iwata M, Mizui Y. *Nat. Chem. Biol.* 2007; 3:570–575. [PubMed: 17643112] Kaida D, Motoyoshi H, Tashiro E, Nojima T, Hagiwara M, Ishigami K, Watanabe H, Kitahara T, Yoshida T, Nakajima H, Tani T, Horinouchi S, Yoshida M. *Nat. Chem. Biol.* 2007; 3:576–583. [PubMed: 17643111] O'Brien K, Matlin AJ, Lowell AM, Moore MJ. *J. Biol. Chem.* 2008; 283:33147–33154. [PubMed: 18826947]
19. Chan DC, Bedford MT, Leder P. *EMBO J.* 1996; 15:1045–1054. [PubMed: 8605874]
20. Bedford MT, Chan DC, Leder P. *EMBO J.* 1997; 16:2376–2383. [PubMed: 9171351] Espejo A, Cote J, Bednarek A, Richard S, Bedford MT. *Biochem. J.* 2002; 367:697–702. [PubMed: 12137563]
21. Harper SJ, Bates DO. *Nat. Rev. Cancer.* 2008; 8:880–887. [PubMed: 18923433]
22. Bates DO, Cui TG, Doughty JM, Winkler M, Sugiono M, J M, Shields D, Peat D, Gillat D, Harper SJ. *Cancer Res.* 2002; 62:4123–4131. [PubMed: 12124351]
23. Woolard J, Wang W–J, Bevan HS, Qiu Y, Morbidelli L, Pritchard-Jones RO, Cui T–G, Sugiono M, Waite RE, Perrin R, Foster R, Digby-Bell J, Shields JD, Whittles CE, Mushens RE, Gillatt DA, Ziche M, Harper SJ, Bates DO. *Can. Res.* 2004; 64:7822–7835.
24. Cébe Suarez S, Pieren M, Cariolato L, Arn S, Hoffmann U, Bogucki A, Manlius C, Wood J, Malner-Hofer K. *Cell Mol. Life Sci.* 2006; 63:2067–2077. [PubMed: 16909199]
25. Perrin RM, Konopatskya O, Qiu Y, Harper S, Bates DO, Churchill AJ. *Diabetologia.* 2005; 48:2422–2427. [PubMed: 16193288]
26. Bates DO, MacMillan DP, Manjaly JG, Qiu Y, Hudson SJ, Bevan HS, Hunter AJ, Soothill PW, Read M, Donaldson LF, Harper SJ. *Clin. Sci. (London).* 2006; 110:575–585. [PubMed: 16451124] Pritchard-Jones RO, Dunn BD, Qiu Y, Varey AH, Orlando A, Rigby H, Harper SJ, Bates DO. *Br. J. Cancer.* 2007; 97:223–230. [PubMed: 17595666]
27. Nowak DG, Woolard J, Amin EM, Konopatskya O, Saleem MA, Churchill AJ, Ladomery MR, Harper SJ, Harper SJ. *J. Cell Sci.* 2008; 121:3487–3495. [PubMed: 18843117]
28. Rennel ES, Waite E, Guan H, Schüler Y, Leenders W, Woolard J, Sugiono M, Gillatt D, Kleinerman ES, Bates DO, Harper SJ. *Br. J. Cancer.* 2008; 98:1250–1257. [PubMed: 18349828]
29. Jurica MS. *Nat. Chem. Biol.* 2008; 4:3–6. [PubMed: 18084270]
30. Kataoka N, Dreyfuss G. *Methods Mol. Biol.* 2008; 488:357–365. [PubMed: 18982302]



**Fig. 1.**  
Structures of borrelidin, analogs and chemical probes.

**Fig. 2.**

**(a)** Four serial rounds of biopanning resulted in the progressive enrichment of two phage products of approx. 450 and 600 bp respectively (highlighted by arrows) as judged by PCR of total phage after each round. The final round was eluted using either SDS (5a) or *E. coli* (5b), and resulted in differential enrichment of these two bands (see right hand image for clarity); **(b)** PCR analysis of single colony isolation of phage from the final round of biopanning (representatives of rounds 5a&b are shown); **(c)** Sequence analysis of the phage PCR products identified a common insert containing a translated 83 amino acid section (red) of FBP21 including its tandem WW domains (underlined) - the translated sequence for a single clone BV14F is shown alongside that for FBP21 (NM\_007187).

**Fig. 3.**

Comparison of the effect of 0.5 and 5  $\mu\text{M}$  **1** and **2** on total VEGF (**a**) and VEGF<sub>xxx</sub>b (**b**) concentrations in RPE cells measured by ELISA, \* $p < 0.05$ , \*\* $p < 0.01$ , Dunnett's compared with vehicle,  $n=3$ ; Insert in **b**) shows PCR for VEGF<sub>165</sub>b in control cells, vehicle treated and cells treated with **2** (**c**) RPE cells treated with increasing concentrations of **2** for 24 h; VEGF<sub>xxx</sub>b and total VEGF concentrations measured by ELISA, \*\* $p < 0.05$ , Dunnett's, \*\* $p < 0.01$ ,  $n=3$ ; (**d**) Effect of IGF-1 and **2** treatment on VEGF<sub>xxx</sub> protein levels; RPE cells were treated with increasing concentrations of **2** and 1  $\mu\text{M}$  IGF-1 for 24 h; total VEGF levels measured by ELISA,  $p=0.0113$ , one way ANOVA, \*\* $p < 0.01$ , Dunnett's compared with IGF alone,  $n=3$ .

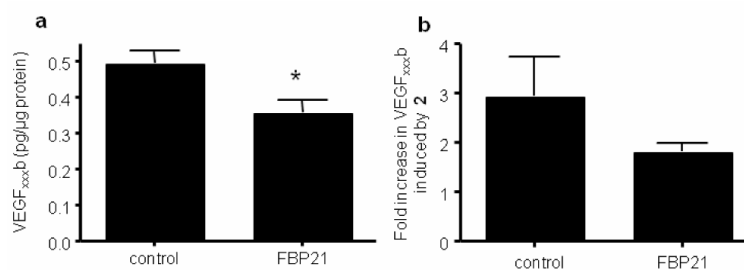


**Fig. 4.** Enhanced FBP21 expression mitigates the effect of **2** on alternative splicing of VEGF in RPE cells. RPE cells were transfected with either control vector or FBP21 expression vector. **(a)** ELISA for VEGF<sub>xxx,b</sub> using biotinylated VEGF<sub>xxx,b</sub> specific detection antibody, \* $p < 0.05$  compared with control, Paired t test,  $n = 3$ ; **(b)** Transfected cells were then treated with  $0.5 \mu\text{M}$  **2** for 72 h and protein assayed by ELISA; results are expressed relative to vehicle (0.1% DMSO) treated cells,  $P = 0.05$  Mann Whitney U test,  $n = 4$ .